

Section I

Cellulose Nanofiber- and Microfiber Based Composites

COPYRIGHTED MATERIAL

1

Cellulose-Nanofiber-Based Materials

Antonio Norio Nakagaito and Hiroyuki Yano

1.1

Introduction

Cellulose is the main constituent of the structural framework of the fibrous cell wall in higher plants, and it is the most abundant polysaccharide in nature. As an organic substance, a considerable fraction of the available carbon in the Earth is sequestered in the cellulose molecules. Among the primary sources of cellulose is wood, with the usual benefits that satisfy the current needs, as being a renewable, sustainable, and carbon-neutral source of biofuels and monomers [1] in addition to cellulose nanofibers. These nanofibers, mostly known as *cellulose microfibrils* by the wood science community, are found embedded in a matrix of hemicelluloses and lignin in the cell wall. The tubular cell wall structure comprises a helically wound arrangement of cellulose microfibrils, nanofibers ($4\text{ nm} \times 4\text{ nm}$) [2] consisting of semicrystalline cellulose molecular chains parallel to their axes. In the crystalline domains, the cellulose chains are arranged in a way such that each long molecule is connected by hydrogen bonds to the neighboring chains forming a highly ordered crystalline form. Every molecule of these chains is made of glucose rings joined together without foldings, just as the benzene rings are joined in aramid. Even the density and the modulus of the two materials are very similar [3]. The cellulose microfibril possesses a Young's modulus close to that of a perfect cellulose crystal, 138 GPa [4], and considering that the strength of a single kraft pulp fiber can reach a tensile strength of 1.7 GPa [5], the estimated tensile strength lays well beyond 2 GPa. That is to say that we can easily find in nature a renewable equivalent of a strong synthetic fiber currently used in aerospace and military applications. It can be obtained from any cellulose source, be it trees, agricultural crops, or even agricultural waste, and if combined with a proper bio-based matrix resin, it has the potential to replace petroleum-based plastics.

This chapter does not intend to be a thorough review of the research activities concerning cellulose nanocomposites, but just aims to introduce the reader to an ebullient field that promises to bring alternatives to the oil-based materials that we became so used to in the past century. More comprehensive surveys can be found in recent review articles by Hubbe *et al.* [6], Siro and Plackett [7], and Moon *et al.* [8].

1.2

The Percolation and Entanglement Phenomena of Cellulose Nanofibers

The reinforcing effect of cellulose nanofibers was extensively studied during the past decade, and as reviewed by Berglund [9], the research concentrated basically on attempts to understand the cellulose microfibril or cellulose whisker reinforcement mechanisms in film composites analyzed in the rubbery state.

The most probable first report on cellulose nanocomposites is attributed by Berglund [9] to Boldizar *et al.* [10]. In 1987, the production of thermoplastics reinforced with hydrolyzed pulp fibers was described. The embrittlement brought by the hydrolytic treatment was intended as a means to facilitate the disintegration of the original fiber into fibrillar entities, or nanofibers, suggesting the possibility to exploit their unusually high modulus and strength values to make composites. Prehydrolyzed cellulose was treated mechanically by a beater or a high-pressure homogenizer, compounded with a thermoplastic matrix (PS (polystyrene)-latex, PP (polypropylene)), and injection molded. The modulus of the composites increased up to three times relative to the pure matrix at a 40 wt% cellulose content, but the tensile strength practically did not change, and in some cases even decreased. The achieved reinforcement was not as high as anticipated because of the possible agglomeration of the fibrils resulting in a poor dispersion inside the matrix. Notwithstanding, PVAC (polyvinyl acetate)-latex mixed with microfibrillated cellulose (MFC) films prepared by casting method revealed the inherent stiffening properties of cellulose microfibrils. Young's modulus of PVAC was improved from 63 MPa to 1.6–2.9 GPa at a 40 wt% cellulose content.

Extensive works involving cellulose microfibrils and whiskers have been carried out by researchers at the Centre de Recherches sur les Macromolécules Végétales—Centre National de la Recherche Scientifique (CERMAV-CNRS), France. In 1995, Favier *et al.* [11, 12] reported the production of polymer films reinforced with cellulose whiskers extracted from sea animals, tunicates. Whiskers are very thin single-crystal fibrils having a nearly perfect crystalline structure. An aqueous suspension of latex obtained by copolymerization of styrene and butyl acrylate was mixed with aqueous suspension of tunicin whiskers and the water was let to evaporate slowly at room temperature. In this method, whiskers were well dispersed throughout the composite. Films up to 6 wt% of cellulose exhibited an increase in shear modulus in the rubbery state of more than two orders of magnitude. Moreover, while the modulus of the matrix decreased with temperature, the modulus of the composites remained constant up to the temperature at which cellulose started to decompose. The unusually large reinforcing effect was explained assuming that a strong interaction between whiskers occurs and is governed by a percolation mechanism, forming a rigid network linked by hydrogen bonds. Helbert *et al.* [13] used the same latex reinforced with whiskers extracted from wheat straw. Water suspensions of latex and whiskers were mixed and freeze dried and then hot pressed. Above the glass-transition temperature (T_g), a 30 wt% whisker composite had a storage modulus of almost two orders of magnitude higher than the matrix. The higher extent of reinforcement was again attributed to

the formation of a whisker network. Chazeau *et al.* [14–16] produced plasticized polyvinyl chloride (PVC) reinforced with tunicin whiskers. Aqueous suspensions of whiskers and microdispersions of PVC were mixed and freeze dried. Then the freeze-dried powder plus plasticizer were hot mixed and compression molded into sheets. The shear elastic modulus at 380 K (above T_g) for a sample with whisker volume content of 12.4% increased almost two orders of magnitude relative to the modulus of the matrix. However, the modulus did not stabilize over T_g , having a decreasing slope similar to that of the matrix materials. In this case, the formation of a flexible whisker network connected by an interphase of immobilized matrix was assumed, instead of a rigid network linked by hydrogen bonds, as a consequence of the processing method by hot mixing and compression. Dufresne *et al.* [17] produced elastomeric Mcl-PHA (medium-chain-length poly(hydroxyalkanoate)) latex reinforced with tunicin whiskers. The storage tensile modulus of a 6 wt% whisker content composite above T_g increased almost an order of magnitude compared to the matrix. Similar to the previous case, the reinforcing effect was attributed to the formation of a whisker network connected by transcrystalline layers grown on cellulose surface instead of a rigid network because of the semicrystalline nature of the matrix.

Other research reporting the production of composites reinforced with tunicin whiskers using different matrix materials, such as PHO (poly(β -hydroxyoctanoate)) [18], resulted in the storage modulus drop above T_g being reduced from 3 GPa for the matrix to 0.5 GPa for a film reinforced by 6 wt% whiskers; and epoxy [19], where storage modulus above T_g for a 2.5 wt% whisker was 38 MPa compared to that of the matrix, 1.9 MPa. In both cases, the formation of a rigid network of hydrogen-bond-linked whiskers reinforcing the composites was observed. Further research was reported with reinforcing whiskers of chitin instead of cellulose, which showed varied results regarding the formation of whisker networks. Chitin is another abundant polysaccharide found in the exoskeleton tissue of marine crustaceans and insects. The chemical structure of chitin is identical to that of cellulose except that a hydroxyl group on each glucose ring is replaced with an acetamido group [20]. Poly(caprolactone) matrix composites [21] exhibited a partial formation of whisker networks, while latex matrix composites [22] showed formation of rigid networks. The reinforcement by chitin whiskers of natural rubber [23, 24] showed that only the casting method leads to the formation of whisker networks while freeze drying and hot pressing does not. Only the slow evaporation process gives enough time for whiskers to move and form a rigid network within the matrix. Chemical modification of the surface of chitin whiskers [25] improved their adhesion to the natural rubber matrix but led to a decrease in mechanical properties of the composites, indicating a partial or complete avoidance of the chitin whisker network formation. Yet, all these studies attribute the reinforcing effect of the whisker-filled composites to the formation of a percolated network.

In a percolated system, all the reinforcing elements are connected in a way such that there are paths linking one element to the next forming an unbroken cluster spanning the whole material from edge to edge. In other words, the reinforcing phase of the composite forms some sort of a stiff skeleton that firmly supports

the matrix, rather than a multitude of individual reinforcing elements. These elements could be strongly connected by hydrogen bonds or less strongly by other means depending on the processing of the composite. Evaporation methods from aqueous suspensions seem to preferentially produce hydrogen bondings.

While whisker-filled composites were considered as model systems to enable theoretical predictions, microfibrils were also used as reinforcements. In a communication [26] in 1996, Dinand *et al.* reported the extraction of MFC from sugar beet pulp and later described a more thorough analysis of these microfibril suspensions [27]. The parenchymal cell cellulose could be disrupted by high-pressure homogenization yielding aqueous suspensions of nonflocculating individual or bundles of cellulose microfibrils. Dufresne *et al.* [28] produced films by evaporation casting of aqueous suspension of sugar beet pulp microfibrils. They concluded that the individualization of microfibrils by the mechanical treatment leads to the formation of a network of microfibrils inside the material, similar to what happened to cellulose whiskers. In the following research [29, 30], Dufresne reinforced plasticized potato starch with potato parenchymal microfibrils and improved thermal stability (modulus stabilization above T_g) and water sensitivity, which were typical drawbacks of starch. Above T_g , a modulus increase of about two orders of magnitude was reported even at a filler content of just 5 wt%. But when Angles and Dufresne [31, 32] produced composites filling plasticized starch with tunicin whiskers, it was observed that the reinforcing effect was very low compared to the previous whisker-filled composites. For instance, the storage modulus of a 25 wt% whisker at 365 K (above T_g) was just about 20 times higher than that of the matrix. It was postulated that plasticizing agents such as glycerol and water hindered the formation of hydrogen bonded network within the matrix. However, this result disagrees with the high reinforcing effect of plasticized starch filled with cellulose microfibrils [29]. Hence, they concluded that the differences were due to the differences in flexibility, that is, stiff and straight whiskers in contrast to flexible hairy microfibrils. They suggested that in composites with whiskers, the reinforcing effect is based on the formation of hydrogen bonded network, whereas for composites with microfibrils, the reinforcement is accomplished by the rigid network and also by an entangling effect. The entangling effect of microfibrils was confirmed in a more recent study by Samir *et al.* [33]. An aqueous suspension of latex obtained by copolymerization of styrene and butyl acrylate was mixed with aqueous suspension of sugar beet microfibrils and microfibrils hydrolyzed by 20 and 60 wt% aqueous acid solutions. When composites were subjected to tensile test, the highest reinforcing effect was observed for the unhydrolyzed microfibril composite, from 0.2 MPa modulus and 0.18 MPa strength of the matrix to 114 and 6.3 MPa, respectively, of the unhydrolyzed microfibril composite. As the hydrolysis intensity increased, the tensile modulus and the strength of the composite decreased, showing the diminishing effect of entanglements in the reinforcement. This is probably the most interesting finding concerning the morphological differences of cellulose affecting the mechanical properties of composites. It demonstrated that in order to achieve proper reinforcement in nanocomposites, it is not always necessary to progress the extraction of nanofibers to obtain cellulose crystallites, but maintaining the

elements as microfibrils or bundles of microfibrils with lateral dimensions in the nanoscale has the advantage of better reinforcing efficiency and less energy input required to produce the nanofibers.

1.3

Cellulose-Nanofiber-Based Materials

A definite evidence of the MFC reinforcing potential was shown by Yano and Nakahara [34], when they described the production of molded materials based on microfibrillated pulp fibers without any adhesive with a bending strength of 250 MPa. MFC is a commercially available cellulose morphology consisting of cellulose nanofibers in the form of microfibril bundles (details of its extraction are described in Section 1.4). With the addition of only 2 wt% oxidized starch, the yield strain doubled and the bending strength increased to 310 MPa. This unusually high strength was attributed to the interactive forces (hydrogen bonds or van der Waals forces) developed between the nanometer unit web-like network of cellulose fibrils. The initial water content of about 90 wt% of MFC is slowly extracted while applying the molding pressure, and so during drying, the capillary forces of the intervening water being evaporated draw the fibrils together bridging them by hydrogen bonds. Although the process is highly time consuming, it marked the beginnings of completely “green” high-strength cellulose-nanofiber-based materials.

The properties of a composite depend on the properties of their constituents, the matrix and the reinforcing phase, and on the interfacial interaction between them. In other words, basically three factors are of primary importance to composites: the resin properties, the fiber properties, and the fiber/resin interface characteristics [35]. The fiber and matrix are generally made of two chemically distinct materials so that the interface between them often has poor compatibility leading to deficiencies in stress transfer and water uptake. One of the most interesting ways to overcome this issue is perhaps the concept of self-reinforced polymers such as all-PP composites [36]. As both fiber and matrix are made of the same material, the composites are easily recyclable and have excellent interfacial compatibility. The all-cellulose composite, where both fibers and matrix consist of cellulose was first developed by Nishino *et al.* [37]. Inspired by their pioneering studies, Gindl and Keckes [38] produced the first all-cellulose nanocomposite by selectively dissolving the surface of microcrystalline cellulose (MCC) in a solution of *N,N*-dimethylacetamide (DMAc) containing 8 wt% LiCl after dehydrating MCC by successive immersions in ethanol, acetone, and DMAc. The films obtained after removal of the solvent were optically transparent and exhibited a tensile modulus of 13.1 GPa, a strength of 242.8 MPa, and a strain at fracture of 8.6%.

Using different approaches, Gindl and Yano tackled the same problem of interfacial compatibility by obtaining composites comprising different phases of the same material. While Gindl chemically dissolved cellulose to serve as the matrix resin, Yano took advantage of the hydrophilic nature of cellulose to adhere the fibers by hydrogen bonds similar to the approach in paper making. Interestingly, the

cellulose nanopaper made from wood nanofibers developed by Henriksson *et al.* [39] with a tensile modulus of 13.2 GPa, a strength of 214 MPa, and remarkable toughness is also based in cellulose interfibril interactions through secondary bonds and the mechanical properties are quite close to those of Gindl's all-cellulose nanocomposites.

In principle, the ultimate mechanical properties of the individual reinforcing elements is realized when cellulose whiskers are obtained, which are essentially nanorods consisting of cellulose monocrystals. However, if we consider these elements collectively as part of the reinforcing phase, the interaction between them becomes the weakest link. It is important to note that the cellulose nanofibers or cellulose microfibrils are made up of crystalline and amorphous domains, but even in these less ordered regions, the molecular chains are aligned in the axial direction, roughly similar to the threads of a string. Therefore, cellulose in the form of nanofibers is almost as strong as their whisker counterparts but is flexible enough to mutually entangle in addition to the hydrogen bond percolation. This seems to be the reason why researchers have preferentially chosen nanofibers instead of whiskers to make composites.

1.4

Extraction of Cellulose Nanofibers

Lignocellulosic materials are vastly distributed in the form of plants, crops, and primarily trees. Just to illustrate the complexity of the structure in which cellulose nanofibers are found, let us look at single fibers from wood (Figure 1.1). These are hollow tubes made up of cellulose microfibrils cemented by a matrix of hemicelluloses and lignin. Most of the cell wall materials are located in the S2 layer, which consists of a helically wound framework of microfibrils [5], as depicted in Figure 1.1. The extraction of cellulose microfibrils or microfibril bundles, here

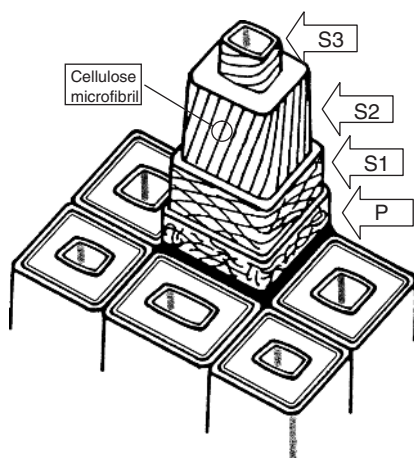


Figure 1.1 The cell wall structure of wood fibers. P is the primary wall; S1, S2, and S3 are the outer, middle, and inner layers of the secondary wall, respectively. (Adapted from a drawing courtesy of Prof. Minoru Fujita.)

referred to as *nanofibers*, is of supreme importance because damage to the elements should be minimal in order to secure the nanoscale diameter and keep the long axial length to preserve the high aspect ratio. The mainstream fibrillation processes reported so far rely on mechanical treatments that subject the fibers to shear forces and they can be summarized in the following methods.

In the early 1980s, a new type of cellulose morphology was developed by Turbak *et al.* [40], called *microfibrillated cellulose (MFC)*. This was a new form of expanded high-volume cellulose, moderately degraded and greatly expanded in surface area, obtained through a homogenization process. Microfibrillation is accomplished in a piece of equipment called *high-pressure homogenizer*, where a dilute slurry of refiner-treated cellulose pulp fibers is pumped at high pressure and fed through a spring loaded valve which opens and closes in a reciprocating motion. The fibers are subjected to a large pressure drop, with shearing and impact forces with the valve seat. The combination of these forces promotes fibrillation and ultimately a high degree of microfibrillation [41]. This cellulose morphology is commercially available and can be considered as consisting of nanofibers as most of the microfibril bundles have submicrometer widths.

Almost two decades later, in the late 1990s, Taniguchi and Okamura [42] reported a process of microfibrillation called super-grinding method. A small commercial grinder with a specially designed super-grinding disk was used to treat a dilute slurry of natural fibers by several passes through the disk. The longitudinal fibrillation is accomplished with very little transverse cutting of the microfibrils, keeping the inherent tensile strength of the fibrils intact and generating a large surface area per unit mass. Iwamoto *et al.* [43] used a similar process to extract cellulose nanofibers to produce optically transparent composites. The starting material was the MFC produced by the high-pressure homogenizer previously developed by Turbak *et al.* [40], further treated by the super grinder to result in more dimensionally uniform nanofibers.

Another method of cellulose microfibrillation was described by Zimmermann *et al.* [44], a disintegration process using a high-speed stirrer and a microfluidizer. In a microfluidizer, a previously split fluid stream containing cellulose are reunited under high pressure in an interaction chamber, where shearing stress is applied to the fibers axis, separating the fibrils. An improvement of the process based on the same principle, called *counter collision in water*, was developed by Kondo [45]. A variation of the use of a microfluidizer, along with a clever enzymatic pretreatment of the fibers, was described by Paakko *et al.* [46]. Instead of a strong acid hydrolysis that produces low aspect ratio elements, a less aggressive enzymatic hydrolysis is used before mechanical fibrillation. After a refiner treatment to increase the accessibility of the enzyme into the cell wall of the fiber, a monocomponent endoglucanase provides selective hydrolysis of the amorphous cellulose regions of the fibers that facilitates a posterior mechanical fibrillation by a high-pressure microfluidizer.

Some creative approaches have been reported of late. Cryocrushing under liquid nitrogen was proposed by Sain's group in Canada [47], where the pulp slurry is pretreated by a fiber disintegrator and a PFI refiner and afterward immersed in liquid nitrogen to freeze the water contained in the interstices of the fibers. The

fibers are subjected to a high impact grinding with a cast iron mortar and pestle to break the fibers cell wall and separate into fibrils. Another interesting method based on mechanical waves was described by Zhao *et al.* [48], which relies on ultrasonication of fibers in aqueous medium. Fibers were fibrillated by applying ultrasound at 20 kHz to various natural fibers composed of silk, chitin, and cellulose. They explained the fibrillation mechanism based on the creation, growth, and collapse of microbubbles in the aqueous solution caused by acoustic cavitation of the high-frequency ultrasound. The shockwaves produced by the collapse of the bubbles causes erosion of the surface of the fibers, splitting them in the axial direction.

Abe *et al.* [49], in an attempt to simplify the grinding method of Taniguchi and Okamura [42] and Iwamoto *et al.* [43], succeeded in fibrillating wood fibers into uniform nanofibers with 15 nm in diameter in only one pass through the grinder, so the damage was the least among the described fibrillation processes (Figure 1.2). In a previous study by Iwamoto *et al.* [50], the severity of mechanical shear applied by the grinder to fibrillate was evaluated based on the mechanical properties of the final nanocomposites. The transparency of composites increased up to five passes through the grinder and beyond that neither transparency nor the morphology of the nanofibers seemed to change. On the other hand, the tensile and thermal expansion properties were significantly degraded, in accordance with the decrease of crystallinity and degree of polymerization of cellulose. Later, they also clarified the role of hemicelluloses on nanofibrillation [51]. According to this study, when the pulp fibers are dried, the presence of hemicelluloses impedes the formation of irreversible hydrogen bonds between microfibrils, known as hornification. And by rewetting, hemicelluloses are plasticized by absorbing water, favoring the ease of posterior nanofibrillation. The essence of Abe's approach was to keep the fiber in a water-swollen state after chemical removal of hemicelluloses and lignin, skipping the drying process in a typical pulp production that causes shrinkage and formation of irreversible hydrogen bonds that mutually adhere the fibrils. This new protocol made possible obtaining perhaps the most undamaged cellulose nanofibers extracted using only mechanical means. This is only rivaled by the nanofibers from never-dried native cellulose obtained by Saito *et al.* [52], who oxidized the surface of the microfibrils by a 2,2,6,6-tetramethylpiperidine-1-oxyl (TEMPO)-radical-catalyzed process, so that just a posterior mechanical agitation by a Waring Blender was enough to individualize the original fibers into nanofibers of 3–5 nm in diameter.

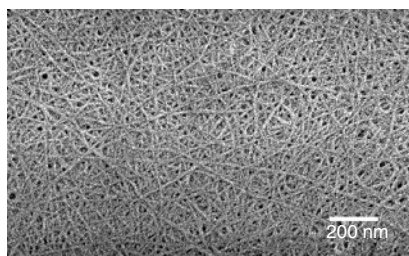


Figure 1.2 Cellulose nanofibers obtained by the grinding treatment from never-dried wood fibers.

In recent times, many new fibrillation processes to obtain nanofibers were developed but still the production yield is low and the energy required to mechanically fibrillate is too high to be economically viable for materials aiming toward their use in commodity products. Perhaps the best approach would be to just obtain a degree of fibrillation to fulfill the needs of each application. For instance, submicrometer fibrils with a broad distribution of lateral sizes would be enough for mechanical reinforcement of composites for semistructural applications, whereas uniform nanofibers with diameters of tens of nanometers (nanofibrillated) would be necessary for optically transparent composites where the nanosized elements are essential for enhanced optical properties. Instead of pursuing the holy grail of perfect fibrillation, different ways to fibrillate will be developed to satisfy the demand in terms of both performance and cost.

1.5

Cellulose-Nanofiber-Based Materials for Structural and Semistructural Applications

Although the utilization of MFC morphology to make high-performance composites was realized rather recently, attempts to exploit the mechanical properties of cellulose microfibrils in strong materials started years earlier. In 1997, Yano *et al.* [53] taking advantage of the high negative correlation between microfibril angle (MFA) and specific Young's modulus in the longitudinal direction of wood, selected raw materials based on sound velocity, hand-picking wood samples containing fibers with the lowest MFAs (Figure 1.1), which gave them the highest modulus and strength. The wood samples were impregnated with a low-molecular-weight phenolic resin and hot pressed at pressures of 30–50 MPa. The resin acted as a plasticizer during compression and after curing, fixed the deformed and densified condition. The Young's modulus and bending strength of the compressed wood achieved values around 40 GPa and 400 MPa, respectively, with some samples exceeding 50 GPa in modulus and 500 MPa in strength for certain species of wood. With a density of only 1.4 g cm^{-3} , such values were comparable to those of soft steel with a density of 7.8 g cm^{-3} or even Duralumin whose density is 2.7 g cm^{-3} . In a subsequent attempt [54], in order to increase the cellulose microfibril content in the composites, the matrix substances were removed by a cyclical treatment in 1 wt% NaClO_2 aqueous solution at 45°C for 12 h followed by rinsing, which was repeated three times to remove lignin, and by soaking in a 0.1 wt% NaOH solution at 20°C for 24 h to extract hemicelluloses. This mild treatment resulted in a total weight reduction of about 30%, the treated veneers were impregnated with phenolic resin and hot pressed as before. Young's modulus and the bending strength increased 48 and 43%, respectively, in relation to the untreated compressed wood, showing that the removal of matrix substances by a mild treatment causing minimal damage to the cellulose microfibrils is an effective way to exploit the strength of cellulose nanofibers. Ultimately, the combination of raw material selection, removal of noncellulosic constituents, and low-molecular-weight phenolic resin impregnation and compression led to the feat of a bending modulus of 62 GPa and a strength of

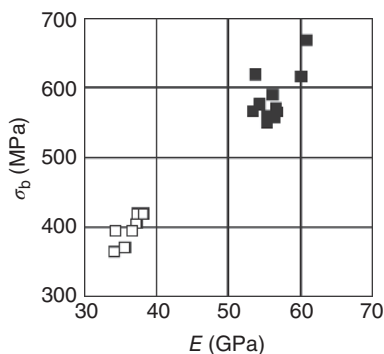


Figure 1.3 Effect of the combination of NaClO_2 and NaOH treatments on the mechanical properties of phenolic-resin-impregnated compressed wood. \square untreated and \blacksquare treated.

670 MPa [55]. Figure 1.3 shows the linear relationship between Young's modulus and bending strength of these composites. Even though these compressed wood composites could not be called *nanocomposites* per se, they are, however, in essence capitalizing on the reinforcing potential of cellulose microfibrils which are nanofibers. Instead of disintegrating wood into individualized fibrils, the original structure of unidirectionally oriented fibers and fibrils of wood was maintained to achieve ultimate strength.

Following the successful attempt by Yano *et al.* [53] to make compressed wood and to utilize the MFC morphology to make strong materials, and considering the good compatibility between cellulose and phenolic resin, sheets similar to paper obtained by filtration of MFC slurries were impregnated with a thermoset resin phenol formaldehyde (PF), stacked in layers and compression molded under pressures as high as 100 MPa [56, 57]. The mechanical properties obtained were substantial, Young's modulus achieved was 19 GPa, and the bending strength attained was about 370 MPa, figures comparable to those of commercial magnesium alloy (Figure 1.4). When compared to composites based on nonfibrillated pulp fibers fabricated following the same compression molding of PF impregnated sheets, MFC nanocomposites had slightly higher Young's modulus but exhibited about 1.5 times higher bending strength. Having similar modulus, the higher bending strength was a direct consequence of a higher strain at fracture of MFC-based composites.

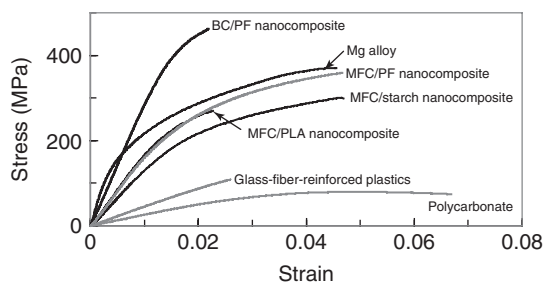


Figure 1.4 Flexural stress-strain curves comparing cellulose nanocomposites with conventional materials.

The enhanced elongation resulted not only in higher strength but also in higher toughness. The work of fracture is attributable to the highly extended surface area of networked nanofibers, which generates an increased bond density that slows down crack propagation. As a consequence of the nanoscale dimensions of the fibrils, fracture sites will be smaller and more widely distributed in the material volume delaying the formation of critical crack necessary for catastrophic failure. The nanostructured material failure is therefore delayed, and the strength is increased.

In order to determine how the degree of fibrillation of kraft pulp reinforcements affects the final composite's strength, samples were produced using wood pulp with different levels of refining and homogenizing treatments [58]. MFC is obtained by repeated mechanical action of a high-pressure homogenizer on wood pulp previously treated by a disk refiner. The number of passes through the homogenizer as well as the number of passes through the refiner determines the degree of fibrillation, resulting in different cellulose morphologies. The degree of fibrillation was evaluated indirectly by water retention values, as it is a physical characteristic related to the exposed surface area of cellulose [40] and serves as an approximate estimate of fibrillation. PF resin was used again as the binder, and the method to produce the composites followed the procedure described earlier. Figure 1.5 shows the bending strength as a function of the degree of fibrillation of pulp fibers, characterized as water retention values. There was no change in strength for composites prepared using pulp fibers treated by refiner up to 16 passes; however, a stepwise increase occurred when the treatment attained 30 passes through the refiner.

Scanning electron microscopy (SEM) observations, as also shown in Figure 1.5, revealed that fibrillation of the fibers surface solely did not increase fiber interactions. Only the complete breakage and fibrillation of the cell wall of the fibers resulted in an increment of mechanical properties, and additional fibrillation by homogenization treatment led to a linear increase of strength. Microfibrillation not only eliminates defects or weaker parts of the original fibers that would act as

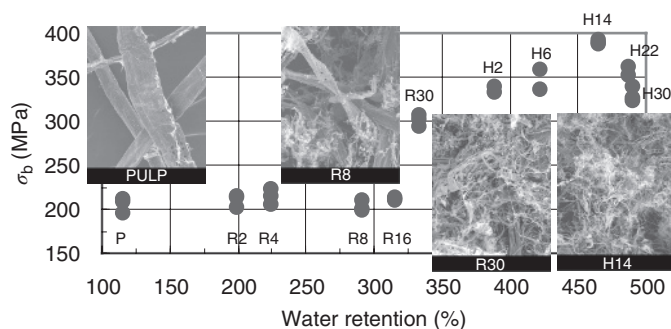


Figure 1.5 Bending strength of composites against water retention of kraft pulp with PF resin contents of 2.4–3.9%. Plots labeled R relate to kraft pulp treated by refiner only, and those labeled H refer to kraft pulp

additionally treated by a homogenizer after 30 passes through the refiner. Numerals denote the number of passes through the refiner or homogenizer.

the starting point of cracks but also increases interfibrillar bond densities, creating a structure that favors ductility.

In a subsequent study, cellulose nanofibers of animal origin instead of plants were utilized by Nakagaito *et al.* [59]. Bacterial cellulose (BC) is secreted extracellularly by *Acetobacter* species cultivated in a culture medium containing carbon and nitrogen sources. It consists of a networked structure of ribbon-shaped pure cellulose fibrils less than 100 nm in width, which in turn are made up of a bundle of finer microfibrils. These fibrils are relatively straight, continuous, dimensionally uniform, and extremely strong, forming a network that macroscopically takes the form of pellicles containing about 99 wt% water. In contrast to MFC, which is obtained in a top-down process by mechanical fibrillation, BC is produced by nature in a bottom-up way, resulting in extremely fine and uniform biosynthesized nanofibers. The composites based on BC were fabricated with sheets obtained from the original BC pellicles by applying pressure to squeeze out the excess water. After drying, the sheets were impregnated with PF resin and compression molded in the same way as with MFC composites. Young's modulus achieved was 28 GPa with bending strength exceeding 400 MPa. Nevertheless, the BC composites were brittle compared to the MFC composites, most likely due to the straight and continuous nanofiber structure contrasting to loose and individualized fibrils of MFC. This was confirmed when BC pellicles were crushed with a grinder, the mechanical properties of composites became very similar to MFC composites, and the fragmented BC morphology observed by SEM revealed to be equally similar to MFC.

All of these materials were fiber-rich composites having high fiber contents up to 70–90 wt%, so an assessment of mechanical properties as a function of fiber content in a wider range was detailed in a later study [60]. Even though the composites based on MFC and PF made by the lamination method have exhibited very good mechanical properties, there was, however, one important deficiency. Because of low resin contents in these fibrous composites and the intrinsic brittleness of PF resin, higher amounts of resin resulted in lower strain at fractures and consequently in lower strengths. Higher resin contents are desirable to make cellulose-based composites less susceptible to degrading agents such as water or moisture. Inspired by studies of Gomes *et al.* [61] and Goda *et al.* [62] that improved the toughness of natural fiber-based microcomposites by alkali treatment of the fibers, the MFC was treated with a strong (20 wt%) NaOH aqueous solution to verify its effectiveness on nanocomposites [63]. As a result of the mercerization of the cellulose nanofibers, the composites with a resin content of about 20 wt% had the strain at fracture increased twice to that of untreated MFC composites with the same resin content. Young's modulus decreased slightly, but the bending strength remained practically unaltered because of the increased strain. Ishikura and Nakano [64] observed that woods treated with strong alkali solutions show reduction in Young's modulus accompanied by a contraction along the fibers direction [65] and surmised that the latter was a direct result of the contraction of the cellulose microfibrils. In the case of mercerized MFC sheets, a similar in-plane contraction was observed. As the lignin in wood hinders the conversion from the crystalline structure cellulose I to cellulose II, Nakano *et al.* [66] proposed that the contraction would be related to an entropy

increase in less ordered regions along the microfibril direction. On that basis, one of the possible explanations for the NaOH-treated MFC composites enhanced ductility might be the straightening of contracted cellulose molecules in amorphous regions when under load. Despite the fact that the real reason is uncertain, the study revealed that only a strong alkali solution treatment results in ductile composites.

1.6

Optically Transparent Materials Reinforced with Cellulose Nanofibers

The current display industry (for TVs, computers, etc.) is largely based on glass-based devices, a market dominated by liquid crystal displays (LCDs), but there is a clear trend toward the development of flexible displays. This new technology offers substantial advantages as the possibility to make displays that are thinner, lighter, robust, and conformable and can be easily rolled away, transported, and stored when not in use. One of the material candidates to replace glass is plastics, but in order to do so plastic substrates have to offer the properties of glass, in addition to being just flexible. One of the major challenges for polymeric substrates is the process temperature required to produce the display panels, thus requiring an extremely low coefficient of thermal expansion (CTE) [67]. The functional materials deposited onto the plastic substrates are susceptible to damage because of the mismatch between the CTEs of the different materials.

A transparent nanocomposite reinforced with BC with high fiber content was reported by Yano *et al.* in 2005 [68]. It was the first example of an optically transparent composite at a fiber content as high as 70 wt%, with a mechanical strength about five times that of engineered plastics, and CTE similar to that of silicon crystal. BC pellicles were compressed to remove the excess water and were afterward dried at 70 °C to completely remove the remaining water. Dried BC sheets were impregnated with acrylic, epoxy, and PF resins. The latter PF resin is a transparent type, different from the previously used PF resin for making high-strength MFC composites. After impregnation, epoxy and acrylic resins were cured by ultraviolet (UV) light and phenolic-resin-impregnated sheets were hot pressed at 150 °C and 2 MPa for 10 min. As the sheets before impregnation had a density of 1.0 g cm⁻³ and considering that the density of cellulose microfibrils is about 1.6 g cm⁻³, the interstitial cavities of BC sheets accounted for about one-third of the sheet's volume. These cavities were filled with transparent thermosetting resins, resulting in final composites with fiber contents between 60 and 70 wt%.

When the light transmittance was measured in the wavelength interval between 500 and 800 nm, the BC/epoxy nanocomposite transmitted more than 80% of the light, surface (Fresnel's) reflection included. Besides, when the transmittance of the BC/epoxy nanocomposite was compared with that of the neat epoxy resin, the reduction in light transmission owing to the reinforcing nanofiber network was less than 10 percentage points. Even considering that for composite materials, the transparency depends primarily on matching the refractive indexes of reinforcing elements and matrix, the BC-reinforced nanocomposite seems to be less sensitive.

The refractive index of cellulose is 1.618 along the fiber and 1.544 in the transverse direction, whereas that of the impregnated epoxy resin is 1.522 at 587.6 nm and 23 °C. Similarly, the refractive indexes of acrylic resins are 1.596 and 1.488 and PF is 1.483, all at 587.6 nm and 23 °C. The high transparency is due primarily to the nanosize effect, that is, elements with sizes much smaller than the wavelength of light prevents its scattering.

Another very attractive property of BC nanocomposites is the unusually reduced thermal expansion. The CTE of the BC/epoxy combination was $6 \times 10^{-6} \text{ K}^{-1}$, an extremely low value compared to $120 \times 10^{-6} \text{ K}^{-1}$ of the epoxy matrix. The CTE of BC/PF was even lower at $3 \times 10^{-6} \text{ K}^{-1}$, a figure as low as that of silicon crystal. The tensile strength measured reached values up to 325 MPa, with Young's modulus around 20–21 GPa. In addition, BC nanocomposites are light, flexible, and easy to mold, making them promising candidate materials for a broad field of applications from flexible displays to windows of vehicles.

In subsequent studies, Nogi *et al.* [69, 70] investigated the performance of these transparent materials under varied circumstances. The extent of the transparency of BC nanocomposites in relation to the refractive index of the acrylic resin was evaluated [69]. It was found that at a wavelength of 590 nm, the total and regular transmittances were above 85 and 75%, respectively, when the refractive index of the resin varied from 1.492 to 1.636. Likewise, the regular transmittance of composites did not vary when the matrix refractive index varied by 0.014 because of the temperature variation from room temperature to 80 °C, showing that the transmittance of composites is stable over a large temperature change making them suitable for a wide range of uses in optoelectronic devices. The evaluation of the BC fiber content in acrylic resin reinforcements [70] revealed that even though the transmittance is linearly reduced with fiber load, it is only reduced by 13.7 percentage points at a fiber content of 66 wt% compared to the neat resin. Meanwhile, the CTE is suppressed drastically with the addition of BC nanofibers, from $86 \times 10^{-6} \text{ K}^{-1}$ of the acrylic resin to just $15 \times 10^{-6} \text{ K}^{-1}$ at around 30 wt% fiber content, further declining to $10 \times 10^{-6} \text{ K}^{-1}$ at 50 wt% fiber load.

As cellulose is highly hygroscopic, moisture absorption by cellulose-based materials is always a primary concern. To address this issue, Nogi *et al.* [71] and Ifuku *et al.* [72] acetylated the BC nanofibers replacing the hydroxyl groups on the surface of the fibers with acetyl groups. As a result, when composites were exposed to a 55% relative humidity at room temperature, the untreated BC composite with 60 wt% fiber content had a moisture content of 3.12%, whereas for the acetylated BC composite, the moisture content was reduced to 1.33% at a fiber loading of 66 wt%. As a plus, other properties were also improved. The CTE of the BC sheet improved from $3 \times 10^{-6} \text{ K}^{-1}$ of untreated to just $0.8 \times 10^{-6} \text{ K}^{-1}$ of the acetylated sheet, even though Young's modulus was reduced from 23.1 to 17.3 GPa. The regular transmittance in one of the BC/acrylic resin combinations revealed that the acetylated BC had increased transparency in the wavelength around 400 nm, maintaining the transparency unaltered in the rest of the visible spectrum. This is a very interesting fact because the authors observed that from SEM images, the untreated BC sheet was densely packed, whereas the acetylated acylated BC sheet

showed nanofibers separated from each other, so that one could speculate that the presence of acetyl groups in the surface of fibrils kept them individualized during drying, hence maintaining the uniformity of the nanosized lateral dimensions of the fibers. Acetylation also brought improved resistance to thermal degradation in terms of optical transparency, the transparency of the acetylated BC nanocomposite subjected to a temperature of 200 °C for 3 h is higher than that of untreated BC nanocomposite exposed to the same temperature for just 1 h.

Another benefit of cellulose nanofiber reinforcement is the enhanced thermal conductivity of the composites. Shimazaki *et al.* [73] reported that epoxy resin reinforced with MFC increased the in-plane thermal conductivity to over $1.0 \text{ W m}^{-1} \text{ K}^{-1}$, a value three to five times higher than that of conventional transparent resins. As the amount of nanofibers was related to the improvement of thermal conductivity and there was no improvement in the direction normal to the in-plane surface, they concluded that the nanofibers are acting as heat pathways to realize high thermal conductivity. Once again the percolated nanofiber network is working favorably to impart additional characteristics to the materials other than optical or mechanical properties.

Later on, the thermal expansion was further decreased in composites with a lower fiber content of just 5 wt%, when BC was combined with a transparent resin having a low Young's modulus [74]. As the modulus of the resin was only 25 MPa, the resulting composite had a modulus of 355 MPa, in the order of high-density polyethylene. This low modulus makes the composite not only flexible but also foldable without damage. Despite the low modulus, the in-plane CTE was unusually low at just $4 \times 10^{-6} \text{ K}^{-1}$. This contradictory phenomenon was explained by the unique structure of BC pellicles, consisting of multiple layers of nanofiber networks that are weakly connected along the thickness direction of the pellicles. Even the low fiber content of 5 wt% is sufficient to restrain the small stresses generated by the expansion of the low modulus matrix in the in-plane direction while in the thickness direction, most of the thermal expansion takes place. This anisotropic behavior makes up for an ultra-low in-plane CTE and also allows enhanced flexibility for the material to be folded without damage.

Even though BC displayed extremely good characteristics to produce transparent composites, the fermentation processes employed to produce BC are overwhelmingly costly for industrial purposes. Therefore, an alternative source of cellulose along with an extraction process that delivers high-quality nanofibers was in great demand at the time. In order to fibrillate wood pulp fibers and reduce the size of fibril bundles to a greater extent, Iwamoto *et al.* [43] complemented the refining/high-pressure homogenization process to obtain MFC with an additional grinding treatment. MFC obtained by 14 passes through the homogenizer has a wide distribution of fibrils width, from some tens of nanometers to some micrometers. As a result, impregnating these MFC sheets with acrylic resin produces transparent composites but not as much as BC/acrylic resin composites. The main reason for this reduced transparency might be attributable to light scattering caused by the larger fibril elements.

As additional passes through the homogenizer did not improve the composites transparency, the 14 passes through homogenizer MFC was subjected to a grinder treatment, realized by 10 iterations. It consists of a mechanical process that applies shearing stresses to the fibers through a commercial grinder fitted out with a pair of specially designed grinding disks. This additional treatment resulted in fibril bundles with dimensions of 50–100 nm in width. This grinder-fibrillated MFC was dispersed in water, and the suspension was vacuum filtered using polytetrafluoroethylene membrane filter, producing a thin sheet. Sheets were oven dried, immersed in neat acrylic resin (tricyclodecane dimethanol dimethacrylate, TCDDMA), and maintained at reduced pressure for 24 h. Impregnated sheets were taken out, and the resin was cured by UV light.

The light transmittance of grinder-fibrillated fiber/acrylic resin composite, pure acrylic resin, BC/acrylic resin, and homogenizer-fibrillated fiber/acrylic resin were measured. At the wavelength of 600 nm, grinder-fibrillated fiber/acrylic composites with 70 wt% fiber content transmitted 70% of light including surface (Fresnel's) reflection. This translates into a transmission reduction of just 20 percentage points compared to the transmittance of the pure acrylic resin. The light transmittance of homogenizer-fibrillated fiber/acrylic composites with 62 wt% fiber content was 30%, or 60 percentage points degraded in relation to the pure resin.

While BC/acrylic resin exhibited the highest transmittance among all the composites, the results also suggested that additional fibrillation of plant fibers might lead to higher light transmittances because the elementary cellulose microfibril is $4\text{ nm} \times 4\text{ nm}$ in cross section, still leaving room for improvements in the fibrillation process. The CTE of the grinder-fibrillated fiber/acrylic resin was measured as $17 \times 10^{-6}\text{ K}^{-1}$, whereas the CTE of the pure acrylic resin is $86 \times 10^{-6}\text{ K}^{-1}$, that is, the grinder-fibrillated nanofibers reduced the CTE of the matrix resin to one-fifth of its original value. Young's modulus was 7 GPa. Although this is lower than the modulus of BC composites, it means more flexibility, they are easier to bend than BC composites.

Okahisa *et al.* [75] reported the fabrication of an optically transparent film made of resin with a low Young's modulus reinforced with cellulose nanofibers extracted from wood. The composite was used as a substrate to deposit an organic light-emitting diode layer. This was a definitive demonstration of the possibilities to produce flexible displays based on plastics reinforced with low cost and sustainable bio-based nanofibers (Figure 1.6).

1.7

Green Cellulose-Nanofiber-Based Materials

As cellulose is a naturally occurring polymer extracted from renewable resources, it is quite intuitive to envisage the possibility to make the resin equally bio-based. The development of MFC composites based on thermoplastics has also been considered, especially in view of the possibility to make completely "green" composites. The polymer of choice was polylactic acid (PLA) and in search for a process that could deliver good dispersion of fibers in the polymer, a quite



Figure 1.6 Foldable BC nanocomposite.

unusual method was devised by Iwatake *et al.* [76]. The water in MFC was replaced by an organic solvent and subsequently mixed with PLA previously dissolved in the same organic solvent. The mixture had the solvent extracted by evaporation, compounded by a kneader, and thin films were obtained by compression molding of the compounds. A 10wt% MFC load resulted in modulus increase of 40% and strength gains of 25% over the neat PLA without a reduction in yield strain. Although the reinforcement effect was explained by the formation of a rigid network of percolated cellulose fibrils, we have to be cautious about this interpretation. In the recent studies by Dalmas *et al.* [77, 78], a latex obtained by copolymerization of styrene and butyl acrylate was mixed with an aqueous suspension of cellulose nanofibers extracted from sugar beet. To make the composites, two different protocols were adopted. The first was through film casting from the suspensions, whereas the second was compression molding of compounds obtained by freeze drying of the original suspension. On the basis of the results of the cyclical tensile tests and swelling experiments among others, they concluded that the casting method resulted in the formation of a rigid network of nanofibers linked by hydrogen bonds, which governs the mechanical properties of the composites. However, such interactions were limited in the case of compression molding, because the viscosity of melted polymer hinders the nanofibril rearrangements, even though some bonds may be created during the process. In the case of PLA and MFC, even if the number of hydrogen bonds would be significantly reduced or even absent, the network should still be present connecting the nanofibers by mutual entanglements instead of secondary bonds. Such fundamental studies are indeed a great help to interpret the reinforcing effects by cellulose nanofibers. Later, Suryanegara *et al.* [79] extended the method to a semicrystalline grade of PLA, succeeding in improving tensile modulus and strength in both amorphous and crystallized states and also enhancing the heat resistance (storage modulus at high temperature), which was not possible with the fully amorphous PLA

grade. The experiments with annealing heat treatments also hinted the possible acceleration of PLA crystallization in the presence of MFC. These findings unveiled the potential of making fully bio-based nanocomposites once new environmentally benign processes are developed.

A great deal of effort has been spent on finding cellulose nanocomposite production routes closer to industrial processes. One of the proposed methods to produce cellulose-nanofiber-reinforced thermoplastics is the twin-screw extrusion compounding of polymer melts, an established process in the plastics industry. This attractive approach has been studied by Oksman's group [80] in Europe in collaboration [81, 82] with Sain's group in North America, especially using PLA for the matrix so as to obtain completely bio-based composites. They have succeeded in reinforcing the polymer at relatively low fiber contents, but with limited success, particularly at high fiber loadings. This is likely due to difficulties in dispersing cellulosic nanofibers in the polymer melt. In general, Young's modulus of composites increased in relation to the neat PLA. However, high fiber contents led to the formation of fiber agglomerations that compromised the ultimate strength of composites. The importance of good dispersion of nanofibers is of major importance, as observed by Takagi and Asano [83]. Oksman and coworkers succeeded in attaining good dispersion of cellulose nanofibers by extrusion adopting a two-step process. A master batch was obtained by dissolving the PLA with a solvent and mixing with cellulose nanofibers at high concentration. Later, the mixture was compounded by a twin-screw extruder, diluting the nanofiber content to 5 wt% and below by addition of PLA. The tensile modulus and strength of neat PLA increased from 2.9 GPa and 58 MPa to 3.6 GPa and 71 MPa, respectively, when composed with 5 wt% nanofibers [84]. Nonetheless, extrusion seems to be one of the very promising ways to fabricate nanofiber-based composites because it is the most common compounding process adopted by the plastics industry. In this kind of processing, perhaps the preferred cellulose morphology should be in the form of nanofibers. While the possibility of the formation of a rigid network by hydrogen bonds is quite reduced [77, 78], in the case of nanofibers, there is still the possibility to obtain a percolated system by entanglements of the long and loose nanofibers. Particularly for these cases, the adoption of low aspect ratio particulates such as MCC or stiffer cellulose whiskers seems not to be much appropriate. Later, a papermaking-like process to obtain sheets from an aqueous suspension of cellulose nanofibers and PLA fibers and subsequently hot press a stack of the dried sheets was proposed [85]. The method is quite simple with potential implementation at an industrial scale.

"Green" nanocomposites also imitate nature. Svagan *et al.* [86], inspired by mechanical properties of plant's cell wall, produced biomimetic nanocomposites by forming a percolated network of cellulose nanofibers in a blend of amylopectin and glycerol by film casting. As the MFC is randomly oriented in plane, a very attractive combination of high strength and high toughness was obtained even at a high fiber content of 70 wt%. Among the reasons, they concluded that the nanofiber network integrity is kept to a strain of at least 8%. In another interesting study [87], biomimetic foams were produced with starch reinforced with MFC by

a lyophilization process. The freezing of the aqueous system of MFC and starch separates the water as the solutes are positioned in the interstices between the ice crystals formed. Sublimation of these ice crystals creates a porous morphology, resulting in strong polysaccharide foams with MFC loads up to 40 wt%, resembling the parenchyma cell in plants.

Besides serving the role of reinforcements, cellulose nanofibers can also make stronger resins. Netravali *et al.* [35] developed modified soy protein concentrates (SPCs) by the addition of MFC. The fracture stress and Young's modulus of these resins are comparable or better than the commonly used diglycidyl ether of bisphenol A (DGEBA)-based epoxy resins. The improved properties are attributed to the strength and aspect ratio of highly oriented and crystalline cellulose molecules in the nanofibers or MFC. These SPC resins combined with natural fibers are the perfect combination to produce high-performance materials which truly are biodegradable end-of-life solutions. The availability of such high-performance thermosets opens up the possibility to substitute PF adhesives to obtain completely bio-based MFC-laminated composites already described in this chapter.

The optically transparent materials described earlier also have matured to the point that it is now completely eco-friendly. The new material is called *cellulose nanofiber paper* by Nogi *et al.* [88], and as the designation suggests, it is made of the same chemical constituents of ordinary paper but with a physical difference in the size of the fibers, the nanofibers obtained by the protocol developed by Abe *et al.* [49], described earlier in this chapter. An aqueous suspension of 0.1 wt% nanofiber was slowly filtered until the water content achieved 560 wt%. The wet sheets were sandwiched between a set of wire meshes, filter paper, and metal plates under a pressure of 15 kPa to avoid wrinkles and dried at 55 °C for 72 h. The density after drying was 1.53 g cm⁻³, quite close to 1.59 g cm⁻³ of the cellulose crystallite [89], indicating that the small interfibrillar cavities were practically eliminated. This was also confirmed by SEM observations. Once the roughness of the surfaces of the sheet was minimized by careful polishing, the transparency at 600 nm wavelength reached 71.6%. The CTE of $8.5 \times 10^{-6} \text{ K}^{-1}$ is comparable to glass. The tensile modulus of 13 GPa and the strength 223 MPa were again very close to the tensile properties reported for all-cellulose nanocomposites of Gindl and Keckes [38] and the cellulose nanopaper of Henriksson *et al.* [39].

This new kind of paper is aimed to be used in all the applications regarding flexible optoelectronics requiring high flexibility, optical transparency, mechanical strength, and low thermal expansion. It is perhaps the ideal “green” substitute for petroleum-based plastics employed thus far.

1.8 Future Prospects

The development of nanocomposites based on the cellulose microfibrils is still in its infancy but is already showing great potential to deliver sustainable materials for a variety of applications, a move away from petroleum. If the current studies

serve as any indication, the next natural step will be without doubt aimed toward the realization of completely “green” cellulose-nanofiber-reinforced composites. However, some really big challenges remain, major one being the need for a really cost-effective means of nanofibrillation. Commodity products demand low cost because it is hard to ask consumers to pay a premium for a new product just based on the environmental advantages brought by a novel technology. Another serious problem is the intrinsic characteristic of cellulose with a strong tendency to aggregate when dried. The ability of the nanofibers to be dried, transported, and redispersed easily in a liquid medium for posterior processing is of paramount importance in terms of market logistics.

Despite the challenges mentioned, the future seems to be bright, as “green” materials are here to stay and to be widely available. Cellulose-based nanocomposites will be one of the alternatives to fulfill the needs of better materials for the coming future.

Abbreviations

BC	bacterial cellulose
CERMAV	Centre de Recherches sur les Macromolécules Végétales
CNRS	Centre National de la Recherche Scientifique
CTE	coefficient of thermal expansion
DGEBA	diglycidyl ether of bisphenol A
DMAc	<i>N,N</i> -dimethylacetamide
LCD	liquid crystal display
LiCl	lithium chloride
MCC	microcrystalline cellulose
Mcl-PHA	medium-chain-length poly(hydroxyalkanoate)
MFA	microfibril angle
MFC	microfibrillated cellulose
NaClO ₂	sodium chlorite
NaOH	sodium hydroxide
PF	phenol formaldehyde
PHO	poly(β -hydroxyoctanoate)
PLA	polylactic acid
PP	polypropylene
PS	polystyrene
PVAC	polyvinyl acetate
PVC	polyvinyl chloride
SEM	scanning electron microscopy
SPC	soy protein concentrate
TCDDMA	tricyclodecane dimethanol dimethacrylate
T_g	glass-transition temperature
UV	ultraviolet

References

1. Beecher, J.F. (2007) *Nat. Nanotechnol.*, **2**, 466–467.
2. O'Sullivan, A.C. (1997) *Cellulose*, **4**, 173–207.
3. Gordon, J.E. (1976) *The New Science of Strong Materials*, Princeton University Press, Princeton, NJ.
4. Nishino, T., Takano, K., and Nakamae, K. (1995) *J. Polym. Sci., Part B: Polym. Phys.*, **33**, 1647–1651.
5. Page, D.H., Elhossei, F., and Winkler, K. (1971) *Nature*, **229**, 252–253.
6. Hubbe, M.A., Rojas, O.J., Lucia, L.A., and Sain, M. (2008) *Bioresources*, **3**, 929–980.
7. Siro, I. and Plackett, D. (2010) *Cellulose*, **17**, 459–494.
8. Moon, R.J., Martini, A., Nairn, J., Simonsen, J., and Youngblood, J. (2011) *Chem. Soc. Rev.*, **40**, 3941–3994.
9. Berglund, L.A., (2005) Cellulose-based nanocomposites in *Natural Fibers, Biopolymers, and Biocomposites* (eds A.K. Mohanty, M. Misra and L.T. Drzal), CRC Press, Boca Raton, FL, USA, pp. 807–832.
10. Boldizar, A., Klason, C., Kubat, J., Naslund, P., and Saha, P. (1987) *Int. J. Polym. Mater.*, **11**, 229–262.
11. Favier, V., Chanzy, H., and Cavaille, J.Y. (1995) *Macromolecules*, **28**, 6365–6367.
12. Favier, V., Canova, G.R., Cavaille, J.Y., Chanzy, H., Dufresne, A., and Gauthier, C. (1995) *Polym. Adv. Technol.*, **6**, 351–355.
13. Helbert, W., Cavaille, J.Y., and Dufresne, A. (1996) *Polym. Compos.*, **17**, 604–611.
14. Chazeau, L., Cavaille, J.Y., and Terech, P. (1999) *Polymer*, **40**, 5333–5344.
15. Chazeau, L., Cavaille, J.Y., Canova, G., Dendievel, R., and Boutherein, B. (1999) *J. Appl. Polym. Sci.*, **71**, 1797–1808.
16. Chazeau, L., Paillet, M., and Cavaille, J.Y. (1999) *J. Polym. Sci., Part B: Polym. Phys.*, **37**, 2151–2164.
17. Dufresne, A., Kellerhals, M.B., and Witholt, B. (1999) *Macromolecules*, **32**, 7396–7401.
18. Dubief, D., Samain, E., and Dufresne, A. (1999) *Macromolecules*, **32**, 5765–5771.
19. Ruiz, M.M., Cavaille, J.Y., Dufresne, A., Graillat, C., and Gerard, J.F. (2001) *Macromol. Symp.*, **169**, 211–222.
20. Stevens, E.S. (2002) *Green Plastics: An Introduction to the New Science of Biodegradable Plastics*, Princeton University Press, Princeton, NJ.
21. Morin, A. and Dufresne, A. (2002) *Macromolecules*, **35**, 2190–2199.
22. Paillet, M. and Dufresne, A. (2001) *Macromolecules*, **34**, 6527–6530.
23. Nair, K.G. and Dufresne, A. (2003) *Biomacromolecules*, **4**, 657–665.
24. Nair, K.G. and Dufresne, A. (2003) *Biomacromolecules*, **4**, 666–674.
25. Nair, K.G., Dufresne, A., Gandini, A., and Belgacem, M.N. (2003) *Biomacromolecules*, **4**, 1835–1842.
26. Dinand, E., Chanzy, H., and Vignon, M.R. (1996) *Cellulose*, **3**, 183–188.
27. Dinand, E., Chanzy, H., and Vignon, M.R. (1999) *Food Hydrocolloids*, **13**, 275–283.
28. Dufresne, A., Cavaille, J.Y., and Vignon, M.R. (1997) *J. Appl. Polym. Sci.*, **64**, 1185–1194.
29. Dufresne, A. and Vignon, M.R. (1998) *Macromolecules*, **31**, 2693–2696.
30. Dufresne, A., Dupeyre, D., and Vignon, M.R. (2000) *J. Appl. Polym. Sci.*, **76**, 2080–2092.
31. Angles, M.N. and Dufresne, A. (2000) *Macromolecules*, **33**, 8344–8353.
32. Angles, M.N. and Dufresne, A. (2001) *Macromolecules*, **34**, 2921–2931.
33. Samir, M.A.S.A., Alloin, F., Paillet, M., and Dufresne, A. (2004) *Macromolecules*, **37**, 4313–4316.
34. Yano, H. and Nakahara, S. (2004) *J. Mater. Sci.*, **39**, 1635–1638.
35. Netravali, A.N., Huang, X., and Mizuta, K. (2007) *Adv. Compos. Mater.*, **16**, 269–282.
36. Peijs, T. (2003) *Mater. Today*, **6**, 30–35.
37. Nishino, T., Matsuda, I., and Hirao, K. (2004) *Macromolecules*, **37**, 7683–7687.
38. Gindl, W. and Keckes, J. (2005) *Polymer*, **46**, 10221–10225.
39. Henriksson, M., Berglund, L.A., Isaksson, P., Lindstrom, T., and Nishino, T. (2008) *Biomacromolecules*, **9**, 1579–1585.

40. Turbak, A.F., Snyder, F.W., and Sandberg, K.R. (1983) *J. Appl. Polym. Sci.: Appl. Polym. Symp.*, **37**, 815–827.
41. Herrick, F.W., Casebier, R.L., Hamilton, J.K., and Sandberg, K.R. (1983) *J. Appl. Polym. Sci.: Appl. Polym. Symp.*, **37**, 797–813.
42. Taniguchi, T. and Okamura, K. (1998) *Polym. Int.*, **47**, 291–294.
43. Iwamoto, S., Nakagaito, A.N., Yano, H., and Nogi, M. (2005) *Appl. Phys. A*, **81**, 1109–1112.
44. Zimmermann, T., Pohler, E., and Geiger, T. (2004) *Adv. Eng. Mater.*, **6**, 754–761.
45. Kondo, T. (2008) *Mokuzai Gakkaishi*, **54**, 107–115.
46. Paakko, M., Ankerfors, M., Kosonen, H., Nykanen, A., Ahola, S., Osterberg, M., Ruokolainen, J., Laine, J., Larsson, P.T., Ikkala, O., and Lindstrom, T. (2007) *Biomacromolecules*, **8**, 1934–1941.
47. Chakraborty, A., Sain, M., and Kortschot, M. (2005) *Holzforschung*, **59**, 102–107.
48. Zhao, H.P., Feng, X.Q., and Gao, H.J. (2007) *Appl. Phys. Lett.*, **90**.
49. Abe, K., Iwamoto, S., and Yano, H. (2007) *Biomacromolecules*, **8**, 3276–3278.
50. Iwamoto, S., Nakagaito, A.N., and Yano, H. (2007) *Appl. Phys. A*, **89**, 461–466.
51. Iwamoto, S., Abe, K., and Yano, H. (2008) *Biomacromolecules*, **9**, 1022–1026.
52. Saito, T., Nishiyama, Y., Putaux, J.L., Vignon, M., and Isogai, A. (2006) *Biomacromolecules*, **7**, 1687–1691.
53. Yano, H., Hirose, A., and Inaba, S. (1997) *J. Mater. Sci. Lett.*, **16**, 1906–1909.
54. Yano, H., Hirose, A., Collins, P.J., and Yazaki, Y. (2001) *J. Mater. Sci. Lett.*, **20**, 1125–1126.
55. Yano, H. (2001) *J. Mat. Sci. Lett.*, **20**, 1127–1129.
56. Nakagaito, A.N., Yano, H., and Kawai, S. (2002) Production of high-strength composites using microfibrillated kraft pulp. Presented at 6th Pacific Rim Bio-based Composites Symposium, Portland, Oregon, 2002.
57. Nakagaito, A.N. and Yano, H. (2005) *Appl. Phys. A*, **80**, 155–159.
58. Nakagaito, A.N. and Yano, H. (2004) *Appl. Phys. A*, **78**, 547–552.
59. Nakagaito, A.N., Iwamoto, S., and Yano, H. (2005) *Appl. Phys. A*, **80**, 93–97.
60. Nakagaito, A.N. and Yano, H. (2008) *Cellulose*, **15**, 555–559.
61. Gomes, A., Goda, K., and Ohgi, J. (2004) *JSME Int. J., Ser. A*, **47**, 541–546.
62. Goda, K., Sreekala, M.S., Gomes, A., Kaji, T., and Ohgi, J. (2006) *Composites Part A*, **37**, 2213–2220.
63. Nakagaito, A.N. and Yano, H. (2008) *Cellulose*, **15**, 323–331.
64. Ishikura, Y. and Nakano, T. (2004) *Mokuzai Gakkaishi*, **50**, 214–219.
65. Ishikura, Y. and Nakano, T. (2007) *J. Wood Sci.*, **53**, 175–177.
66. Nakano, T., Sugiyama, J., and Norimoto, M. (2000) *Holzforschung*, **54**, 315–320.
67. Crawford, G.P. (2005) *Flexible Flat Panel Displays*, John Wiley & Sons Ltd.-Society for Information Display, Chichester.
68. Yano, H., Sugiyama, J., Nakagaito, A.N., Nogi, M., Matsuura, T., Hikita, M., and Handa, K. (2005) *Adv. Mater.*, **17**, 153–155.
69. Nogi, M., Handa, K., Nakagaito, A.N., and Yano, H. (2005) *Appl. Phys. Lett.*, **87**, 1–3.
70. Nogi, M., Ifuku, S., Abe, K., Handa, K., Nakagaito, A.N., and Yano, H. (2006) *Appl. Phys. Lett.*, **88**.
71. Nogi, M., Abe, K., Handa, K., Nakatsubo, F., Ifuku, S., and Yano, H. (2006) *Appl. Phys. Lett.*, **89**.
72. Ifuku, S., Nogi, M., Abe, K., Handa, K., Nakatsubo, F., and Yano, H. (2007) *Biomacromolecules*, **8**, 1973–1978.
73. Shimazaki, Y., Miyazaki, Y., Takezawa, Y., Nogi, M., Abe, K., Ifuku, S., and Yano, H. (2007) *Biomacromolecules*, **8**, 2976–2978.
74. Nogi, M. and Yano, H. (2008) *Adv. Mater.*, **20**, 1849–1852.
75. Okahisa, Y., Yoshida, A., Miyaguchi, S., and Yano, H. (2009) *Compos. Sci. Technol.*, **69**, 1958–1961.
76. Iwatake, A., Nogi, M., and Yano, H. (2008) *Compos. Sci. Technol.*, **68**, 2103–2106.
77. Dalmás, F., Chazeau, L., Gauthier, C., Cavaille, J.Y., and Dendievel, R. (2006) *Polymer*, **47**, 2802–2812.
78. Dalmás, F., Cavaille, J.Y., Gauthier, C., Chazeau, L., and Dendievel, R. (2007) *Compos. Sci. Technol.*, **67**, 829–839.

79. Suryanegara, L., Nakagaito, A.N., and Yano, H. (2009) *Compos. Sci. Technol.*, **69**, 1187–1192.
80. Oksman, K., Mathew, A.P., Bondeson, D., and Kvien, I. (2006) *Compos. Sci. Technol.*, **66**, 2776–2784.
81. Mathew, A.P., Oksman, K., and Sain, M. (2005) *J. Appl. Polym. Sci.*, **97**, 2014–2025.
82. Mathew, A.P., Oksman, K., and Sain, M. (2006) *J. Appl. Polym. Sci.*, **101**, 300–310.
83. Takagi, H. and Asano, A. (2008) *Composites Part A*, **39**, 685–689.
84. Jonoobi, M., Harun, J., Mathew, A.P., and Oksman, K. (2010) *Compos. Sci. Technol.*, **70**, 1742–1747.
85. Nakagaito, A.N., Fujimura, A., Sakai, T., Hama, Y., and Yano, H. (2009) *Compos. Sci. Technol.*, **69**, 1293–1297.
86. Svagan, A.J., Samir, M.A.S.A., and Berglund, L.A. (2007) *Biomacromolecules*, **8**, 2556–2563.
87. Svagan, A.J., Samir, M.A.S.A., and Berglund, L.A. (2008) *Adv. Mater.*, **20**, 1263–1269.
88. Nogi, M., Iwamoto, S., Nakagaito, A.N., and Yano, H. (2009) *Adv. Mater.*, **21**, 1595–1598.
89. Sugiyama, J., Vuong, R., and Chanzy, H. (1991) *Macromolecules*, **24**, 4168–4175.

